Narrow acoustic field of view drives frequency scaling in toothed whale biosonar

Frants H. Jensen[1,2*], Mark Johnson[3,4], Michael Ladegaard[4],
Danuta Wisniewska[4,5], and Peter T. Madsen[4]

[1] Aarhus Institute of Advanced Studies, Aarhus University, 8000 Aarhus C, Denmark
[2] Biology Department, Woods Hole Oceanographic Institution, 266 Woods Hole Rd, Woods Hole, MA 02543, USA
[3] Scottish Ocean Institute, University of St. Andrews, Scotland
[4] Zoophysiology, Department of Bioscience, Aarhus University, 8000 Aarhus C, Denmark
[5] Hopkins Marine Station, Stanford University, CA, USA

***Corresponding author:** frants.jensen@gmail.com

MANUSCRIPT PUBLICATION STATUS:
ACCEPTED in CURRENT BIOLOGY

Summary

Toothed whales are apex predators varying in size from 40-kg porpoises to 50-ton sperm whales that all forage by emitting high-amplitude ultrasonic clicks and listening for weak returning echoes [1, 2]. The sensory field of view of these echolocating animals depends on the characteristics of the biosonar signals and the morphology of the sound generator, yet it is poorly understood how these biophysical relationships have shaped evolution of biosonar parameters as toothed whales adapted to different foraging niches. Here we test how biosonar output, frequency, and directivity vary with body size to understand the co-evolution of biosonar signals and sound-generating structures. We show that the radiated power increases twice as steeply with body mass ($P \propto M^{1.47\pm0.25}$) than expected from typical scaling laws of call intensity [3], indicating hyperallometric investment into sound production structures. This is likely driven by a strong selective pressure for long-range biosonar in larger oceanic or deep-diving species to search efficiently for patchy prey. We find that biosonar frequency scales inversely with body size ($F \propto M^{-0.19\pm0.03}$), resulting in remarkably stable biosonar beamwidth that is independent of body size. We discuss how frequency scaling in toothed whales cannot be explained by the three main hypotheses for inverse scaling of frequency in animal communication [3-5]. We propose that a narrow acoustic field of view, analogous to the fovea of many visual predators, is the primary evolutionary driver of biosonar frequency in toothed whales, serving as a spatial filter to reduce clutter levels and facilitate long-range prey detection.

Keywords (up to 10):
Echolocation, toothed whales, evolution, phylogenetic comparative methods, foraging, ecology, biosonar directivity, field of view, frequency scaling

Current Biology Highlights (85 characters per highlight, incl space; up to 4 highlights):

- Toothed whales have evolved four different biosonar signals for echolocating prey
- Larger whales echolocate with higher output levels and at lower click rates
- Inverse frequency scaling leads to relatively conservative directivity
- Biosonar frequency is driven by a need for a highly directional field of view

eTOC blurp (350 characters incl spaces):

Jensen et al. analyse scaling of echolocation signal parameters in toothed whales to unravel the evolutionary drivers of biosonar operation. They show that large species use lower frequency and higher source levels for longer prey detection range, but have remarkably similar beamwidth to small species. This suggests that a narrow field of view may drive inverse frequency scaling in animal biosonar.

Results and discussion

Toothed whales and bats, constituting one-fifth of all mammalian species, navigate and find prey using echolocation in which they emit high-intensity acoustic signals and listen for returning echoes [1, 2]. Toothed whales comprise 75 species of apex predators that have adapted to a highly diverse set of feeding niches ranging from flooded forests and river systems to mesopelagic depths of the deep ocean. Toothed whales depend on a pneumatic sound generator in their nasal passages to generate ultrasonic echolocation signals [6, 7], which include the most intense acoustic signals found in animals [8]. Morphological features associated with biosonar sound production suggest that echolocation may have evolved shortly after the split between toothed and baleen whales some 32 mya [9]. Although it is debated whether high-frequency hearing or echolocation evolved first [10-12], there is both paleontological and genetic evidence that evolution of ultrasonic hearing occurred rapidly at the base of the toothed whale radiation [13, 14].

While the origin of toothed whale echolocation is reasonably clear, the diversification of toothed whale biosonar clicks and its consequences for sonar performance in different foraging niches has received much less attention. Extant toothed whales use four types of biosonar search clicks (Fig. 1): Sperm whales (*Physeteriidae*) produce broadband clicks that reverberate within the head to produce a multi-pulsed (MP) click [8]. Beaked whales (*Ziphiidae*) produce frequency-modulated (FM) clicks [15, 16]. Most delphinoids and river dolphins rely on a simple broadband (BB) click [17], whereas porpoises, franciscana dolphin, pygmy and dwarf sperm whales, and six species from the *Lagenorhynchus* and *Cephalorhyncus* genera generate narrowband high-frequency (NBHF) clicks [18-20] (Fig. 1, Table S1). Despite large-scale differences in frequency and bandwidth, it remains poorly understood how evolution has shaped biosonar parameters in parallel with changes in body size. Sound source parameters of terrestrial animals have been better studied, showing that larger animals generally produce communication signals at higher source levels [3] and at lower frequencies [4] compared to small animals, leading to a number of proposed scaling rules for animal communication signals. However, while animals typically broadcast communication signals in all directions, directional signals are beneficial for echolocation. Since signal frequency directly affects both sound directivity and attenuation,

and therefore the sensory volume in which echolocating predators can detect prey [21], such traditional scaling laws may work differently for echolocating animals. Here we use phylogenetic regression of biosonar parameters of toothed whales to identify the evolutionary drivers of biosonar operation and to test whether predictions from scaling of animal communication signals hold for echolocating toothed whales.

Hyperallometric scaling of sound production structures lead to increasing biosonar output for large whales

Toothed whales produce sound using a specialized set of nasal sound generators termed the phonic lips [6]. Sound production is driven by air pressure in the lower nasal passages set up by muscular activation of the nasopharyngeal pouch [7]. The radiated acoustic power is likely limited by both the muscles responsible for the driving air pressure and by the size of the vibrating phonic lips, both of which scale with the size of the animal [7], resulting in increasing biosonar output with body size (Fig. 2A). If toothed whales invest a constant fraction of their metabolic energy into sound production, then we expect the radiated acoustic power to scale with body mass to the power of ¾ following studies of terrestrial animals [3]. In toothed whales, this assumption does not seem to hold: The radiated acoustic power per click (P, in Watts) increases twice as steeply with body size (Fig. 2B-D) as expected from the ¾ power scaling rule (pGLS: $P \propto M^{1.47\pm0.25}$; table 1), indicating hyperallometric growth of sound-producing structures. This is likely closely tied to increasing cranial asymmetry. Most toothed whales have two sets of phonic lips, with the right pair typically used for echolocation [22, 23]. Both delphinids and ziphiids exhibit significant cranial asymmetry [24] with a larger right compared to left set of phonic lips [6]. However, porpoises and other NBHF species, that are generally small, show little to no cranial asymmetry [25] and employ a relatively low peak-power biosonar [18-20] which they partially compensate for by producing longer echolocation signals with higher total energy. On the other end of the size scale, sperm whales have a uniquely enlarged nasal complex with only a single hypertrophied right pair of phonic lips that in turn allows them to produce extremely powerful biosonar clicks [8]. This hyperallometric investment in

sound generating structures means that toothed whales as a whole do not abide by the typical scaling laws of animal call intensity [3].

Biosonar search range increases with body size

As a consequence of increasing sound source levels, larger animals greatly increase their prey detection range and sensory volume under noise-limited conditions (Fig. 2E). Prey detection range for an echolocating animal can be estimated either through acoustic modelling [26, 27] or by using biosonar click rates as a proxy for the maximum inspection range [17, 28]. Across toothed whales, estimated target detection range, assuming identical prey and spectral noise, increases from tens of meters for NBHF species up to hundreds of meters for large ziphiids and sperm whales (Fig. 2E). While prey size and background noise certainly differ across species, these increases in detection range are mirrored by systematic differences in maximum inspection range of free-ranging animals (Fig. 2F). Since echolocating predators typically wait for echoes to return before emitting the next click, larger animals clicking slower may indicate that they are searching for prey at greater distances. The systematic increase in maximum prey detection range relative to body length results in larger animals being able to probe a greater volume of water for prey. This may be extremely important for oceanic and deep-diving animals that traverse large distances in search of patchy prey [29] , and where foraging performance depends on the time it takes to find patches or evaluate patch quality. In contrast, the short detection range of shallow-water or riverine species is likely an adaptation to habitats where reverberation or clutter [30], rather than noise, may limit effective prey detection [31, 32]. Thus, peak output levels and biosonar sampling rates reflect large-scale sensory adaptations to different foraging niches that are themselves tied into the size and hence diving capabilities of the animal.

Inverse scaling of biosonar frequency driven by narrow acoustic field of view

Large terrestrial animals generally vocalize at lower sound frequencies compared to smaller animals [33], and many studies have sought to identify the underlying principles

behind frequency scaling in animal communication. Fletcher et al. [4], Bennet-Clark [34] and Bradbury and Vehrenkamp [33] have argued that call frequency should be inversely proportional to body length (thereby resulting in $F \propto M^{-1/3}$) to ensure efficient sound production, since efficiency decreases sharply when the wavelength of emitted sound becomes larger than the circumference of the sound source [4]. Fletcher [5, 35] developed a more general model integrating sound production, propagation, and reception to estimate the sound frequency that maximizes communication range. With this functional approach, optimum frequency should scale with a slightly steeper power law for terrestrial animals ($F \propto M^{-0.40}$) and a much steeper power law for aquatic animals due to more efficient sound propagation ($F \propto M^{-0.60}$). Finally, Gillooly and Ophir [3] examined the possibility that maximum sound frequency is constrained by the rate of individual muscle contractions and concluded that frequency should therefore scale with a lower coefficient ($F \propto M^{-0.25}$) [3].

Our results for toothed whales show a clear frequency scaling with size (Fig. 3A) that initially seems to support the muscle contraction model given very similar power law coefficients (pGLS: $F \propto M^{-0.19\pm0.03}$; table 1). However, the biosonar frequencies of toothed whales are orders of magnitude higher than predicted from the frequency scaling relationship of communicating terrestrial mammals [34]. Furthermore, echolocation clicks are produced pneumatically [7], meaning that the muscle contraction hypothesis may be a poor causal explanation for inverse frequency scaling in toothed whales. The higher frequency compared to terrestrial animals of similar body size partially relates to the higher sound speed in water, meaning that efficient sound pressure radiation requires approximately 4.5 times higher sound frequency for the same sound generator size. However, Fletcher's [4] sound production efficiency hypothesis also does not seem applicable since echolocating toothed whales use frequencies that are 10-30 times higher than required for efficient sound production.

An alternative ecological driver that might explain the high biosonar frequencies relates to the reflectivity of small prey [36, 37]; to achieve efficient backscatter, the dominant wavelength of the biosonar pulse should be less than the circumference of the target [38],

meaning that minimum biosonar frequencies could be determined by the smallest prey of interest. In addition, if prey discrimination for target selection is required, frequencies must be well above this limit to generate detailed spectral information about target properties in the returning echo. An argument against the prey backscatter hypothesis is that NBHF species show no scaling of frequency with size. These four groups of animals have independently evolved NBHF biosonar signals with centroid frequency around 130 kHz, likely to avoid killer whale predation [39, 40]. While small NBHF species use biosonar frequencies close to those predicted by scaling of frequency with body size, larger NBHF species use frequencies that are much higher than predicted for their size (Fig. 3A) and we find no significant scaling of frequency within NBHF species (Fig. 3B).

Finally, biosonar frequency also has consequences for other aspects of echolocation. Frequency, biosonar directivity and the size of the sound emitter are tightly coupled in echolocating animals [41] so that transmitting directivity increases with the product of sound frequency and emitter size (i.e., the size of the melon). This makes it imperative to consider the implications of frequency choice on the directivity and therefore the field of view. We find a remarkable convergence on a narrow biosonar beam with a high directivity index (DI = 26±2 dB: Fig. 3B) for wild toothed whales covering two orders of body mass (pGLS: R2 = 0.01, $F_{1,17}$ = 0.16, p = 0.69). This convergence mirrors similar patterns observed for trained bats [41] and raises the question of whether selection pressures are acting primarily on frequency or field of view. Paradoxically, NBHF species that show no scaling of biosonar frequency with body size still use biosonar beams with similar directivity [18-20], meaning that transmitter aperture or melon size needs to be disproportionally small for larger NBHF species. Thus, at least in NBHF species, a narrow acoustic field of view does not seem to be a passive consequence of improving reflectivity of prey. In these species, a narrow field of view may have driven co-evolution of smaller transmitting apertures along with increasing biosonar frequency for larger NBHF species, suggesting that the acoustic field of view by itself may have evolutionary benefits.

The evolutionary benefits of a narrow acoustic field of view

Our finding that free-ranging toothed whales spanning three orders of magnitude in body mass have converged on a high biosonar directivity (Fig. 3D) suggests that the resulting narrow field of view may confer direct fitness advantages that can drive the co-evolution of biosonar parameters and structures associated with sound production and beam focusing in toothed whales. Several advantages of a narrow acoustic field of view may explain this remarkable sensory convergence:

For a power-limited biosonar system, an increase in transmitting directivity results in a longer and narrower field of view ahead of the echolocating whale (biosonar detection hypothesis). This enables longer detection range of individual or patchy prey under conditions where ambient noise limits echo detection, while also increasing time for planning captures [26].

The spatial filtering realised by a narrow acoustic field of view simultaneously reduces the generation of unwanted echoes from other objects in the environment [42], easing the cognitive demands [43] required to process complex acoustic scenes (spatial filtering hypothesis). This further facilitates biosonar operation in acoustically complex, cluttered or highly reverberant areas such as coastal or riverine environments or in polar pack ice.

A narrow field of view may also help in tracking prey (prey tracking hypothesis) by providing rapid changes in echo level as the narrow sonar beam is used to scan across the prey, as proposed for bats [44].

Given these potential benefits, it is reasonable to ask why toothed whales do not have even narrower fields of view than the observed 5 to 10 degrees beamwidth. Several trade-offs may be at work here. First, while a narrow field of view increases source level and on-axis detection range, the total volume ensonified per click decreases with increasing directivity (since ensonified volume V is proportional to the square root of the biosonar beamwidth). Animals might partly compensate for this through movements that sequentially scan a wider swath, thus gaining the benefit of a long detection range and a large search volume [45]. A narrow field of view and correspondingly high SL also results in an average

detection distance that increases with directivity (since detection distance is proportional to $1/\sqrt{\theta}$). Consequently, the time to intercept prey increases, thereby potentially reducing the number of prey captures per unit time but providing longer time for planning approaches and prey capture. A final problem posed by a narrow biosonar beam is analogous to the "homicidal chauffeur" problem from game theory [46]; during close-quarter prey tracking, prey only have to make relatively small excursions perpendicular to the axis of a narrow beam to escape the field of view. To some degree, toothed whales may have already addressed this problem since both phocoenids [47], iniids [32, 48], and delphinids [49] all demonstrate some level of dynamic control over their field of view by increasing beamwidth during target approach.

Conclusion

In conclusion, we have shown that size is an important factor shaping the biosonar output and detection range of toothed whales but not their acoustic field of view. Hyperallometric investment in sound production organs in toothed whales means that the scaling coefficient of biosonar power to body mass is significantly higher than for animal communication signals. Consequently, larger whales can detect prey at longer range, and they click slower to inspect these more distant regions. Conversely, there is a remarkable convergence on narrow biosonar beams across species independent of body size that mirrors similar patterns in bats and may be analogous to the optical foveas of visual predators. We argue that the ecological advantages of a narrow field of view for biosonar-based prey search may drive both an inverse scaling of biosonar frequency with size, at frequencies much higher than typical animal communication signals, and the co-evolution of sound transmitter morphology. An optimal acoustic field of view, independent of body size, may be a trade-off between long-range prey detection and clutter reduction, balanced against an increasingly small ensonified volume and larger risk of prey escaping the sensory field.

Author contributions:

FHJ and PTM conceived the paper, FHJ and ML gathered and curated data, FHJ and DMW performed analyses, FHJ created visualizations with input from DMW, MJ, ML and PTM, FHJ and PTM drafted manuscript, all authors revised manuscript.

Acknowledgements:

We would like to thank Jeremy Goldbogen and Will Gearty for advice on phylogenetic scaling analysis and Larry Foster for use of illustrations. FHJ received support from a Carlsberg Foundation travel grant and an AIAS-COFUND fellowship from Aarhus Institute of Advanced Studies. ML was funded by a PhD stipend from the Faculty of Science and Technology, Aarhus University, and National Research Council grants to PTM. DMW was supported by the Danish National Research Foundation and Carlsberg Foundation grants to PTM. MJ was partly supported by an Aarhus University visiting professorship.

References:

1. Schevill, W.E., and McBride, A.F. (1956). Evidence for echolocation by cetaceans. Deep Sea Research (1953) *3*, 153-154.
2. Griffin, D.R. (1958). Listening in the dark: the acoustic orientation of bats and men, (New Haven CT: Yale University Press).
3. Gillooly, J.F., and Ophir, A.G. (2010). The energetic basis of acoustic communication. Proc. R. Soc. Lond., B, Biol. Sci. *277*, 1325-1331.
4. Fletcher, N.H. (1992). Acoustic Systems in Biology, (New York: Oxford University Press).
5. Fletcher, N.H. (2004). A simple frequency-scaling rule for animal communication. J Acoust Soc Am *115*, 2334-2338.
6. Cranford, T.W., Amundin, M., and Norris, K.S. (1996). Functional morphology and homology in the odontocete nasal complex: Implications for sound generation. J Morphol *228*, 223-285.
7. Ridgway, S.H., and Carder, D.A. (1988). Nasal pressure and sound production in an echolocating white whale, *Delphinapterus leucas*. In Animal Sonar: Processes and Performance, P.E. Nachtigall and P.W.B. Moore, eds. (New York and London: Plenum), pp. 53-60.
8. Møhl, B., Wahlberg, M., Madsen, P.T., Heerfordt, A., and Lund, A. (2003). The monopulsed nature of sperm whale clicks. J Acoust Soc Am *114*, 1143-1154.
9. Geisler, J.H., Colbert, M.W., and Carew, J.L. (2014). A new fossil species supports an early origin for toothed whale echolocation. Nature *508*, 383-386.
10. Fahlke, J.M., Gingerich, P.D., Welsh, R.C., and Wood, A.R. (2011). Cranial asymmetry in Eocene archaeocete whales and the evolution of directional hearing in water. Proc Natl Acad Sci *108*, 14545-14548.

11. Ekdale, E.G., and Racicot, R.A. (2015). Anatomical evidence for low frequency sensitivity in an archaeocete whale: comparison of the inner ear of Zygorhiza kochii with that of crown Mysticeti. J Anat *226*, 22-39.
12. Park, T., Fitzgerald, E.M., and Evans, A.R. (2016). Ultrasonic hearing and echolocation in the earliest toothed whales. Biol Lett *12*.
13. Churchill, M., Martinez-Caceres, M., de Muizon, C., Mnieckowski, J., and Geisler, Jonathan H. (2016). The Origin of High-Frequency Hearing in Whales. Curr. Biol.
14. Liu, Y., Rossiter, S.J., Han, X.Q., Cotton, J.A., and Zhang, S.Y. (2010). Cetaceans on a molecular fast track to ultrasonic hearing. Curr. Biol. *20*, 1834-1839.
15. Johnson, M., Madsen, P.T., Zimmer, W.M.X., de Soto, N.A., and Tyack, P.L. (2004). Beaked whales echolocate on prey. Proc. R. Soc. Lond., B, Biol. Sci. *271*, S383-S386.
16. Johnson, M., Madsen, P.T., Zimmer, W.M.X., de Soto, N.A., and Tyack, P.L. (2006). Foraging Blainville's beaked whales (*Mesoplodon densirostris*) produce distinct click types matched to different phases of echolocation. J Exp Biol *209*, 5038-5050.
17. Au, W.W.L. (1993). The Sonar of Dolphins, (New York: Springer Verlag).
18. Kyhn, L.A., Jensen, F.H., Beedholm, K., Tougaard, J., Hansen, M., and Madsen, P.T. (2010). Echolocation in sympatric Peale's dolphins (*Lagenorhynchus australis*) and Commerson's dolphins (*Cephalorhynchus commersonii*) producing narrow-band high-frequency clicks. J Exp Biol *213*, 1940-1949.
19. Kyhn, L.A., Tougaard, J., Beedholm, K., Jensen, F.H., Ashe, E., Williams, R., and Madsen, P.T. (2013). Clicking in a killer whale habitat: Narrow-band, high-frequency biosonar clicks of harbour porpoise (*Phocoena phocoena*) and Dall's porpoise (*Phocoenoides dalli*). PLoS ONE *8*, e63763.
20. Kyhn, L.A., Tougaard, J., Jensen, F., Wahlberg, M., Stone, G., Yoshinaga, A., Beedholm, K., and Madsen, P.T. (2009). Feeding at a high pitch: Source parameters of narrow band, high-frequency clicks from echolocating off-shore hourglass dolphins and coastal Hector's dolphins. J Acoust Soc Am *125*, 1783-1791.
21. Jakobsen, L., Kalko, E.V., and Surlykke, A. (2012). Echolocation beam shape in emballonurid bats, *Saccopteryx bilineata* and *Cormura brevirostris*. Behav Ecol Sociobiol *66*, 1493-1502.
22. Madsen, P.T., Lammers, M., Wisniewska, D., and Beedholm, K. (2013). Nasal sound production in echolocating delphinids (*Tursiops truncatus* and *Pseudorca crassidens*) is dynamic, but unilateral: clicking on the right side and whistling on the left side. The Journal of Experimental Biology *216*, 4091-4102.
23. Madsen, P.T., Wisniewska, D., and Beedholm, K. (2010). Single source sound production and dynamic beam formation in echolocating harbour porpoises (*Phocoena phocoena*). J Exp Biol *213*, 3105-3110.
24. Wood, F.G., and Evans, W.E. (1980). Adaptiveness and ecology of echolocation in toothed whales. In Animal Sonar Systems, R.G. Busnel and J.F. Fish, eds. (New York: Plenum), pp. 381-426.
25. Yurick, D.B., and Gaskin, D.E. (1988). Asymmetry in the Skull of the Harbor Porpoise Phocoena-Phocoena (L) and Its Relationship to Sound Production and Echolocation. Canadian Journal of Zoology-Revue Canadienne De Zoologie *66*, 399-402.
26. Au, W.W.L. (2014). Dolphin biosonar target detection in noise: Wrap up of a past experiment. J Acoust Soc Am *136*, 9-12.

27. Madsen, P.T., Wilson, M., Johnson, M., Hanlon, R.T., Bocconcelli, A., Aguilar de Soto, N., and Tyack, P.L. (2007). Clicking for calamari: toothed whales can echolocate squid *Loligo pealeii*. Aquat. Biol. *1*, 141-150.
28. Thomas, J.A., and Turl, C.W. (1990). Echolocation characteristics and range detection thresholds of a false killer whale (*Pseudorca crassidens*). In Sensory abilities of Cetaceans: Laboratory and field evidence, J.A. Thomas and R.A. Kastelein, eds. (Springer).
29. Fais, A., Soto, N.A., Johnson, M., Perez-Gonzalez, C., Miller, P.J.O., and Madsen, P.T. (2015). Sperm whale echolocation behaviour reveals a directed, prior-based search strategy informed by prey distribution. Behav Ecol Sociobiol *69*, 663-674.
30. Au, W.W.L., and Turl, C.W. (1983). Target detection in reverberation by an echolocating Atlantic bottlenose dolphin (*Tursiops truncatus*). J Acoust Soc Am *73*, 1676-1681.
31. Jensen, F.H., Rocco, A., Mansur, R.M., Smith, B.D., Janik, V.M., and Madsen, P.T. (2013). Clicking in Shallow Rivers: Short-Range Echolocation of Irrawaddy and Ganges River Dolphins in a Shallow, Acoustically Complex Habitat. PLoS ONE *8*, e59284.
32. Ladegaard, M., Jensen, F.H., de Freitas, M., Ferreira da Silva, V.M., and Madsen, P.T. (2015). Amazon river dolphins (*Inia geoffrensis*) use a high-frequency short-range biosonar. J Exp Biol *218*, 3091-3101.
33. Bradbury, J.W., and Vehrenkamp, S.L. (1998). Principles of acoustic communication, (Sunderland, MA: Sinauer Associates).
34. Bennet-Clark, H.C. (1998). Size and scale effects as constraints in insect sound communication. Philosophical Transactions of the Royal Society B: Biological Sciences *353*, 407-419.
35. Fletcher, N.H., and Index, A. (2005). Acoustic systems in biology: from insects to elephants. Acoustics Australia *33*, 83.
36. Schnitzler, H.U., and Kalko, E.K.V. (2001). Echolocation by insect-eating bats. Bioscience *51*, 557-569.
37. Houston, R.D., Boonman, A.M., and Jones, G. (2004). Do echolocation signal parameters restrict bats' choice of prey? In Echolocation in bats and dolphins, J.A. Thomas, C.F. Moss and M. Vater, eds. (Chicago, IL: University of Chicago Press), pp. 339-345.
38. Clay, C.S., and Medwin, H. (1977). Acoustical Oceanography, (New York: Wiley-Interscience).
39. Andersen, S.H., and Amundin, M. (1976). Possible predator-related adaptation of sound production and hearing in the Harbour porpoise. Aquat. Mamm. *4*, 56-57.
40. Morisaka, T., and Connor, R.C. (2007). Predation by killer whales (*Orcinus orca*) and the evolution of whistle loss and narrow-band high frequency clicks in odontocetes. J. Evol. Biol. *20*, 1439-1458.
41. Jakobsen, L., Ratcliffe, J.M., and Surlykke, A. (2013). Convergent acoustic field of view in echolocating bats. Nature *493*, 93-96.
42. Simmons, J.A., Kick, S.A., Moffat, A.J.M., Masters, W.M., and Kon, D. (1988). Clutter interference along the target range axis in the echolocating bat, Eptesicus-fuscus. J Acoust Soc Am *84*, 551-559.
43. Dukas, R. (2004). Causes and Consequences of Limited Attention. Brain, Behavior and Evolution *63*, 197-210.
44. Yovel, Y., Falk, B., Moss, C.F., and Ulanovsky, N. (2010). Optimal Localization by Pointing Off Axis. Science *327*, 701-704.

45. Shaffer, J.W., Moretti, D., Jarvis, S., Tyack, P., and Johnson, M. (2013). Effective beam pattern of the Blainville's beaked whale (*Mesoplodon densirostris*) and implications for passive acoustic monitoring. J Acoust Soc Am *133*, 1770-1784.
46. De Villiers, R., Miloh, T., and Yavin, Y. (1988). Stochastic pursuit-evasion differential games in 3D: The case of variable speed. Journal of Optimization Theory and Applications *59*, 25-38.
47. Wisniewska, D.M., Ratcliffe, J.M., Beedholm, K., Christensen, C.B., Johnson, M., Koblitz, J.C., Wahlberg, M., and Madsen, P.T. (2015). Range-dependent flexibility in the acoustic field of view of echolocating porpoises (*Phocoena phocoena*). eLife, 2015; 2010.7554/eLife.05651.
48. Ladegaard, M., Jensen, F.H., Beedholm, K., da Silva, V.M.F., and Madsen, P.T. (2017). Amazon river dolphins (*Inia geoffrensis*) modify biosonar output level and directivity during prey interception in the wild. The Journal of Experimental Biology.
49. Jensen, F.H., Wahlberg, M., Beedholm, K., Johnson, M., de Soto, N.A., and Madsen, P.T. (2015). Single-click beam patterns suggest dynamic changes to the field of view of echolocating Atlantic spotted dolphins (*Stenella frontalis*) in the wild. The Journal of Experimental Biology *218*, 1314-1324.

Figure legends:

Figure 1: Evolution and diversification of biosonar signal types in toothed whales

A: Biosonar signal types mapped onto the molecular phylogeny of odontocetes (adapted from McGowen *et al.* 2009). Rectangles, color-coded by biosonar signal type, represent the ten families of extant toothed whales. B-E: Waveforms of on-axis biosonar search signals for four representative species: *Physeter macrocephalus* (B; red), *Ziphius cavirostris* (C; blue, *Phocoena phocoena* (D; purple) and *Tursiops aduncus* (E; yellow). F: Normalized power spectra corresponding to waveforms. G: Quality factor Q_{rms} (defined as the centroid frequency divided by the root-mean-square (RMS) bandwidth) vs click centroid frequency for on-axis biosonar signals.

Figure 2: Biosonar output and detection range increases with body size

A: Source level in energy flux density as a function of body mass for toothed whales, with source level of wild animals typically measured using acoustic arrays (insert). Grey lines: Power law relationship (solid) and 95% confidence intervals (dashed) estimated using phylogenetic generalized least squares. Notable outliers (pGLS λ estimated to 0) are marked with species name, alphabetically: *Chea: Cephalorhynchus heavisidii; Dl: Delphinapterus leucas; Gg: Grampus griseis; Gma: Globicephala macrorhynchus; Gme: Globicephala melas; Md: Mesoplodon densirostris; Oo: Orcinus orca; Pp: Phocoena phocoena.* B-D: Log-power vs log-body mass plots with phylogenetically corrected regression lines (grey solid lines) and 95% confidence intervals (grey dashed lines) for all toothed whales (B), NBHF species (C) and broadband delphinid species (D). Black line represents the theoretical $P \propto M^{3/4}$ relationship expected for animals that invest a constant fraction of metabolic energy into sound generating structures (Gillooly and Ophir 2010). E: Estimated prey detection range for a noise-limited scenario modelled from biosonar output parameters, target properties and background noise using the active sonar equation (SL: Source level; TL: Transmission loss; TS: Target strength; EL: Echo level; R: Range; Au, 1993) (see Supplemental Experimental Procedures). F: Echolocating predators generally process returning echoes from targets of interest before emitting subsequent clicks since

this allows for range estimation. A proxy for the maximum inspection range can therefore be estimated from interclick intervals (listening time), assuming a fixed neural processing time of 20 ms (Au, 1993) irrespective of species. G: Correlation between estimated maximum target detection and inspection range.

Figure 3: Inverse scaling of biosonar frequency leads to narrow field of view across species

A-C: Log-centroid frequency vs log-body mass plots with pGLS regression (solid lines) and 95% CI (dashed lines) across all odontocetes (A), for NBHF species (B) and for BB species (C). D: Sonar beam directivity index DI (the difference between on-axis source level and a theoretical source level if energy was radiated equally in all directions; see also Table S1) plotted as a function of body size, with pGLS regression (solid lines) and 95% CI (dashed lines). In both plots, species towards the extremes have been labelled with species abbreviation, alphabetically: *Dl: Delphinapterus leucas; Gm: Globicephala macrorhynchus; Ha: Hyperoodon ampullatus; Kb: Kogia breviceps; Lal: Lagenorhynchus albirostris; Lau: Lagenorhynchus australis; Md: Mesoplodon densirostris; Mm: Monodon Monoceros; Pd: Phocoena dalli; Pg: Platanista gangetica gangetica; Pm: Physeter macrocephalus; Sc: Sousa chinensis; Ta: Tursiops aduncus*. Right panels: Composite vertical beam pattern (normalized relative to on-axis sound level) reconstructed from measured DI and representative on-axis clicks for four representative odontocete species: *Physeter macrocephalus* (E), *Ziphius cavirostris* (F), *Tursiops aduncus* (G) and *Phocoena phocoena* (G). Drawings used with permission by Larry Foster.

Figures:

Figure 1: Evolution and diversification of biosonar signal types in toothed whales

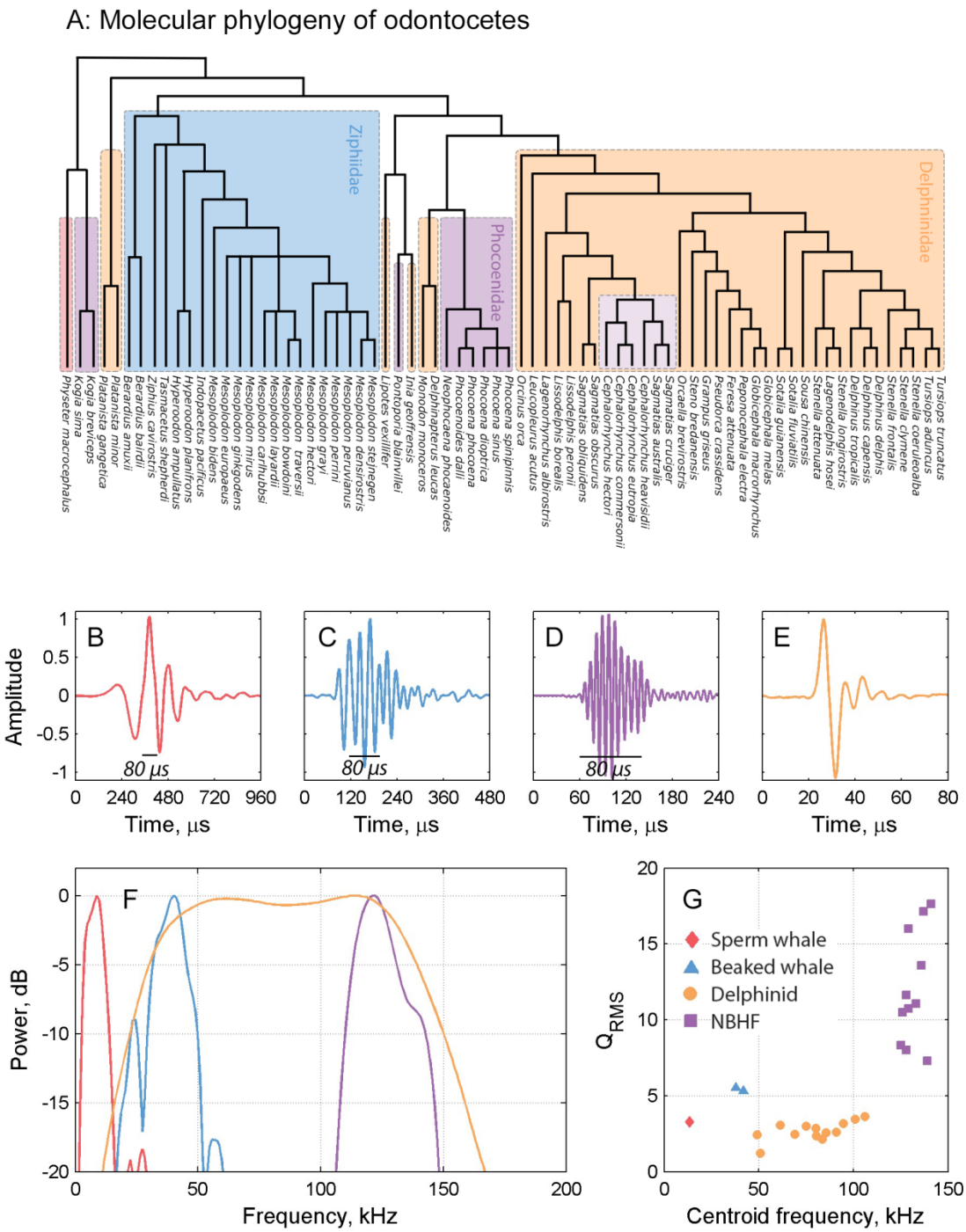

Figure 2: Biosonar output and detection range increases with body size.

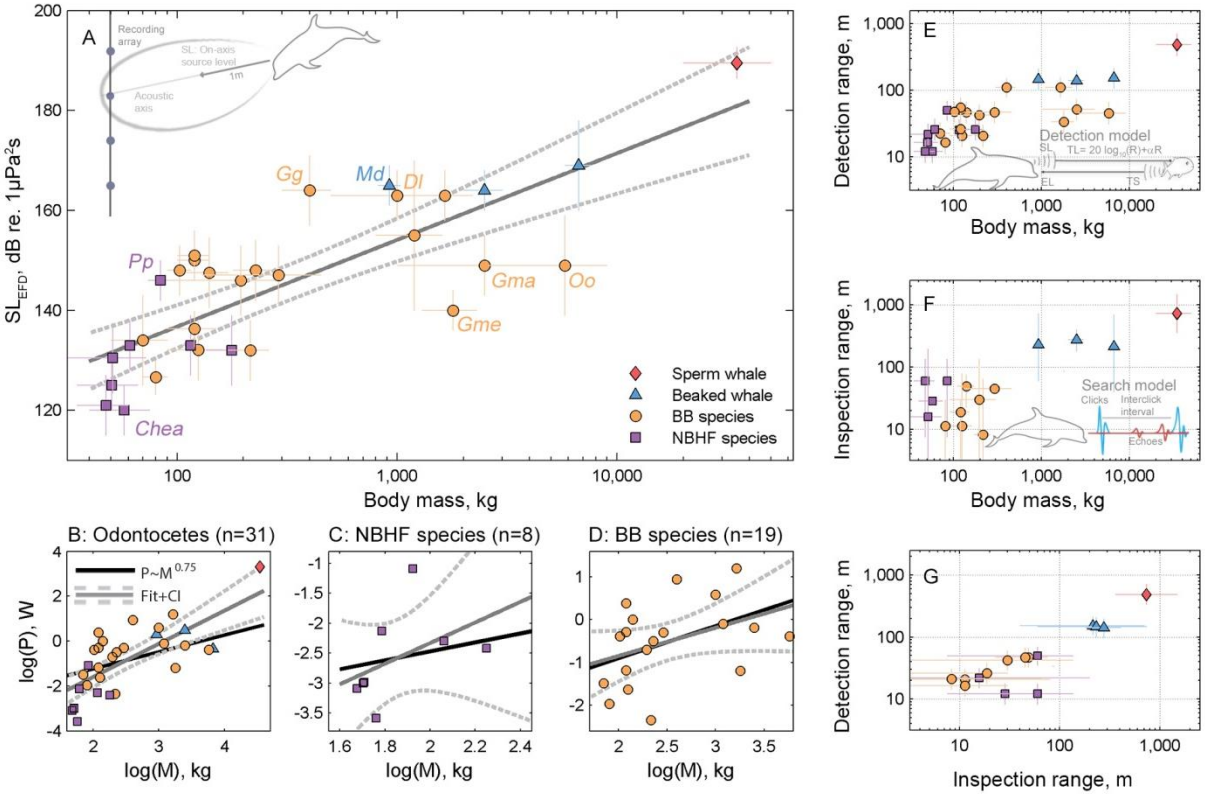

Figure 3: Inverse scaling of biosonar frequency leads to narrow field of view across species

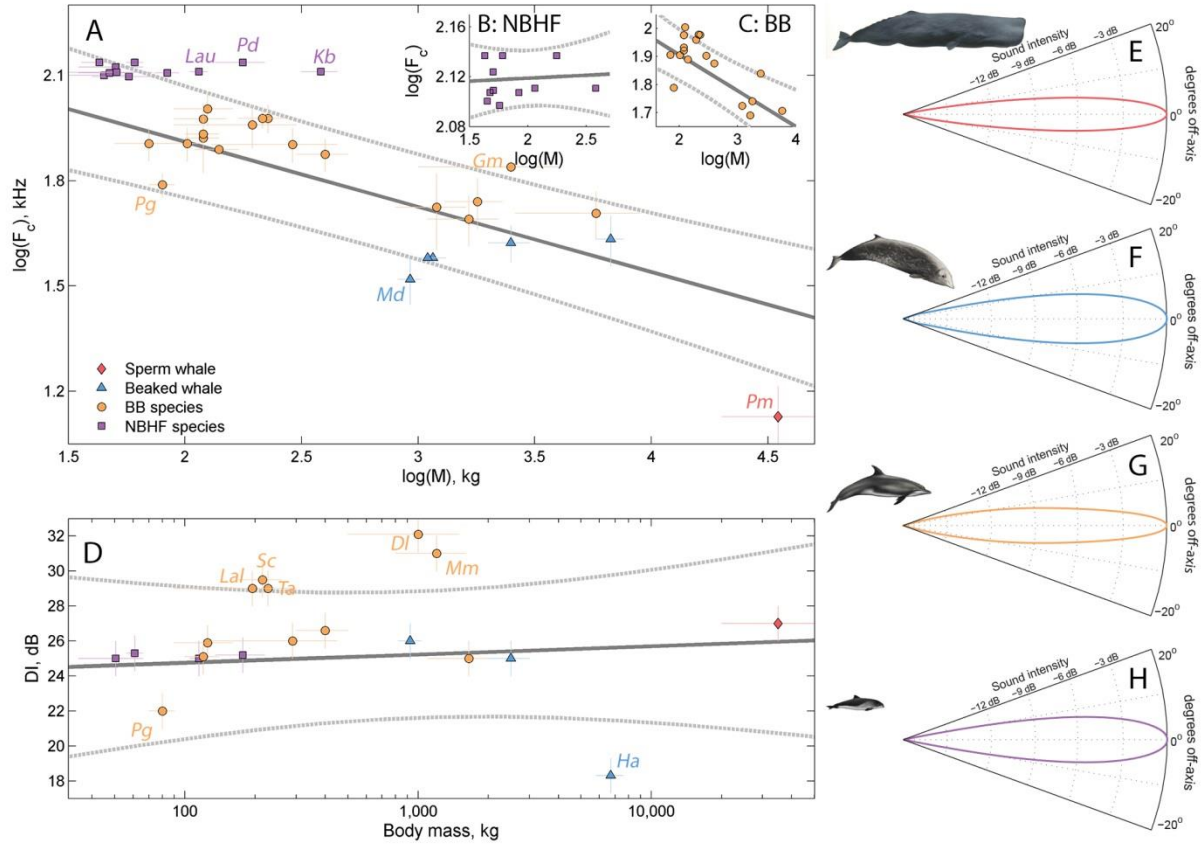

Table 1: Phylogenetic generalized least squares (pGLS) analysis of toothed whale biosonar parameters. For each analysis, Pagel's λ was estimated using the *pgls* function in the *caper* R package to account for phylogenetic signal. After adjusting branch lengths for a possible phylogenetic signal, scaling coefficients (reflecting a power relationship to body mass M in the form $Y \propto aM^b$) are reported as mean ± standard error along with 95% confidence intervals.

Relationship between biosonar output level and body size: *PGLS model:* $EFD = b\ ln(M)$							
Species	**pGLS λ**	**Scaling coefficient b**	**95% CI**	**R^2**	**F**	**df**	**p**
Odontocetes	0	17.35±2.38 dB	[12.7 : 22.0]	0.65	53.15	1,29	***5.0*10^{-8}***

Relationship between biosonar power and body size: *PGLS model:* $Log_{10}(P) = b\ log_{10}(M)$							
Species	**pGLS λ**	**Scaling coefficient b**	**95% CI**	**R^2**	**F**	**df**	**p**
Odontocetes	0	1.47±0.25	[0.97 : 1.97]	0.53	33.29	1,29	***3.0*10^{-6}***
NBHF species	0	1.72±1.37	[-0.95 : 4.40]	0.20	1.58	1,6	0.26
BB species	0	0.65±0.37	[-0.06 : 1.38]	0.16	3.21	1,17	0.09

Relationship between biosonar frequency and body size: *PGLS model:* $Log_{10}(F_c) = b\ log_{10}(M)$							
Species	**pGLS λ**	**Scaling coefficient b**	**95% CI**	**R^2**	**F**	**Df**	**p**
Odontocetes	**0.932**	-0.19±0.03	[-0.25 : -0.13]	0.49	31.74	1,33	***2.8*10^{-6}***
NBHF species	**0.674**	-0.00±0.02	[-0.04 : 0.03]	0.01	0.08	1,9	0.78
BB species	**0.551**	-0.13±0.03	[-0.18 : -0.07]	0.55	19.71	1,16	***0.0004***

Relationship between biosonar directivity and body size: *PGLS model:* $DI = b\ log_{10}(M)$							
Species	**pGLS λ**	**Scaling coefficient b**	**95% CI**	**R^2**	**F**	**Df**	**p**
Odontocetes	**0.839**	0.47±1.17 dB	[-1.44 : 3.12]	0.01	0.16	1,17	0.69